

OPTIMIZATION OF RF CAVITIES USING MOGA FOR ALS-U*

H. Feng^{†1}, T. Luo, D. Li, K. Baptiste, Lawrence Berkeley National Laboratory, Berkeley, CA, USA
W. Huang, Ch. Tang, Z. Liu, Department of Engineering Physics, Tsinghua Uni, Beijing, China
¹also at Department of Engineering Physics, Tsinghua University, Beijing, China

Abstract

A multi-objective genetic algorithm-based optimization process has been applied to optimize the RF design of a 500 MHz main cavity and a 1.5 GHz Higher Harmonic Cavity (HHC) for the Advanced Light Source upgrade (ALS-U) in Lawrence Berkeley National Laboratory (LBNL). For the main cavity, a significant improvement, compared with the existing ALS cavity, has been achieved in cavity shunt impedance and power loss density simultaneously. The field strengths and distribution of the optimized structure are analysed for further research. For the HHC, a cavity with low R/Q has been preliminary designed to mitigate the beam instability. This study also serves as an example of how a genetic algorithm can be used for optimizing RF cavities.

INTRODUCTION

The ALS-U conceptual design promises to deliver diffraction limited performance in the soft x-ray range by lowering the horizontal emittance to about 70pmrad resulting in two orders of brightness increase for soft x-rays compared to the current ALS [1]. A multiyear upgrade includes new and replacement x-ray beamlines, a replacement of many of the original insertion devices and many upgrades to the accelerator.

The multi-objective genetic algorithm NSGA-II is adopted to search for the optimal structure of the cavity design. For the 500 MHz main cavity, the optimization process is accomplished by varying the 8 geometry knobs. Simultaneously optimizing the two competing objectives, shunt impedance and power density, better-performed structures are found. After boundary hitting check and data analysis, optimization based on former good results are implemented and the structures are further studied. An optimum of 13.34% for shunt impedance and reduction of max power density up to 39.2% are found in the results.

In terms of the physics requirement of the higher harmonic cavity of ALS-U, a preliminary required-low R/Q design and optimization has been carried out to mitigate the beam instability. This method is also previously applied in APEX-II gun cavity optimization [2].

ALGORITHM DESCRIPTION

As for RF cavity design and optimization, starting from a known structure and calculating the corresponding characteristics are the general steps. In comparison, algorithm-

based optimization inversely begins from the desired characteristics and generates the controllable cavities parameters which meet with the requirements.

During the past decades, many different algorithms based on MOGA [3] emerge to improve both computational speed and complexity. The general steps include the assignment of initial population, implementation of crossover and mutation, a suitable standard for selection and the repetition of above procedures. Among them, Non-dominated Sorting Genetic Algorithm-II (NSGA-II) [4] perform great excellence in computational complexity, using an explicit diversity preserving mechanism and emphasizing on non-dominated solutions. Due to the nature of NSGA-II, running parallel with 100% efficiency on any number of processors is achievable to greatly improve the calculation speed.

OPTIMIZATION OF THE MAIN CAVITY

For the main RF cavity, the goal of optimization is to increase the shunt impedance R_S while keeping max power dissipation density P_m under a certain range. After revising the top part of the cavity from circle to ellipse, as is shown in Fig. 1, the 8 geometry variables in clockwise direction are: the horizontal radius of ellipse r_{1a} , the vertical radius of ellipse r_{1b} , side wall length l_1 , inner corner angle θ_1 , inner corner radius r_2 , nose cone height h , nose cone radius r_3 , beam pipe radius l_3 . As for other indirect variables, nose cone radius $\theta_2 = \theta_1 - 90^\circ$ and nose cone side wall length $l_2 = h/\sin \theta_2$ are relevant with the direct variables. The length of RF cavity (for synchronism considerations between RF phase and beam) and the mesh thickness for calculation are carefully chosen and fixed.

In comparison with the measured results of 5 M Ω [5], a slight difference is shown due to the engineering and mechanical reasons. The simulation result of ALS original cavity is taken as the calibration standard in optimization. The Poisson/SUPERFISH [6] is used to calculate the geometry and characteristics of the RF cavity. As the definitions goes:

$$Z = \frac{\int_0^L E_z(z) dz}{PL} \quad (1)$$

Where P is the total power loss, L is the length of the structure, E_z is the amplitude of the electric field intensity on-axis. Combined with the definition in the original papers of ALS [5], we calculate the effective shunt impedance as $R_S = Z \cdot T^2 \cdot L$, in which T is the transit-time factor. R_S is obtained by multiply R/Q and Q in SUPERFISH output and P_m can be extracted directly from the output results. Because of the symmetry of the cavity structure, quarter cavity geometry is adopted for simulation to lift the calculation

* Work supported by the Director of Office of Science of the U.S. Department of Energy under Contract No. DE-AC02-05CH11231
[†] hfeng@lbl.gov

Content from this work may be used under the terms of the CC BY 3.0 licence (© 2019). Any distribution of this work must maintain attribution to the author(s), title of the work, publisher, and DOI

speed. After loads of testing, the appropriate numbers of generation and population are chosen. Running parameters are listed in Table 1.

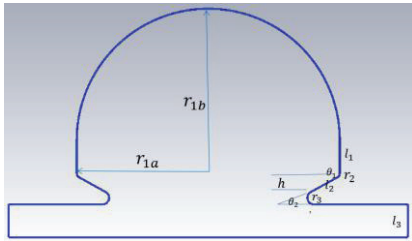


Figure 1: Cavity cell with optimized geometry variables.

This multi-objective optimization problem becomes:

- Objectives:
 - ① Maximize shunt impedance R_S ,
 - ② Minimize max power density P_m
- Constrains:
 - ① Frequency f within the range of 504 +/-3 MHz,
 - ② $Q > 40000$, ③ $E_{max} < 15$ MV/m

Table 1: The Running Parameters of the Program

Parameters	Values
Population size	360
Generation	50-100
Probability of crossover	0.8
Probability of mutation	0.3

Pareto Front Analysis

With the stochastic process going through, the objectives fluctuate during the computation and some unphysical structures occur. The results converge to Pareto Front gradually as generations go by as Fig. 2 shows. We first take shunt impedance as the priority and look into the acceptable max power density. Several candidates are chosen as listed in Table 2.

The first geometry (g1) has the largest increase on shunt impedance while power density rises sharply at the same time. The last geometry (g3) is chosen because its same performance on shunt impedance as the original one, however the power density is much lower surprisingly. As a trade-off, g2 is chosen for deeper exploration. The electromagnetic field distribution is shown in Fig. 3.

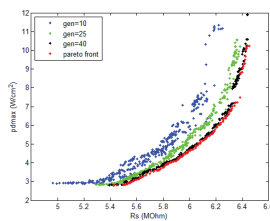


Figure 2: The convergence to Pareto front.

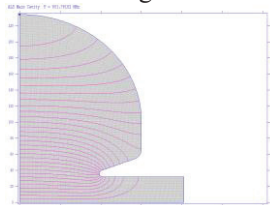


Figure 3: Electromagnetic field distribution of g2.

Table 2: Representatives Chosen from Pareto Front

Parameters	Original	g1	g2	g3
f (MHz)	504.34	501.27	501.76	501.12
R_S (M Ω)	5.63	6.44	6.38	5.63
		(+14.4%)	(+13.3%)	(0)
P_m (W/cm ²)	5.20	10.32	7.97	3.21
				(-38.3%)
Q	45719	41188	43686	48996
R/Q (Ω)	123.37	156.34	145.95	114.99
E_{max} (MV/m)	7.53	11.51	10.57	7.74

A boundary hitting check on the parameters of the geometries separately is performed to see the above well-performed structures' parameters distribution in the searching range. The values of the normalized parameters are scaled from 0 to 1. For the selected structures, r_{1a} reaches the boundary obviously. Figure 4 (left) is an example shown using g2. To gain a clearer view on the parameter distribution, the final convergence of parameters (using the values of Pareto front) is analysed. Figure 4 (right) presents how four parameters vary with shunt impedance as a demonstration.

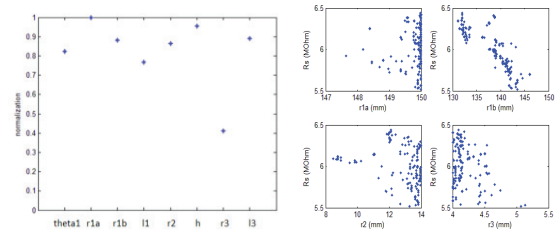


Figure 4: (left) Boundary hitting check of parameters for g2. (right) Influence of parameters from new Pareto front on objectives (using four parameters as a demonstration).

Further Improvement

Steps from the following aspects are taken to further optimize the results:

1. Continue the above calculation steps reusing the previous computed Pareto front as the new initial generation.
2. Narrowing the searching range of certain parameters. (Both perspectives conserve computation efficiency.)
3. Enlarging the searching range of variables which already hit the border.
4. Adjusting the probability of crossover and mutation.

Based on the former results, some new and better performed geometries occur as is listed in Table 3. G1 to G3 are selected for the same reasons as g1 to g3. G2 has the same R_S as g2 while the maximum power density is reduced. Since G2 and G3 out-perform g2 and g3, they are focused for further study. Characteristics of G2 present the optimal result for the whole process.

Discussion

3D structures are tested in CST Microwave studio [7]. To explore the specialty of the structure in-depth, the difference of E field between G2 and the original design, and

the difference of H field between G3 and the original design are analysed (see Fig. 5).

Table 3: Representatives Chosen from Pareto Front in the Improvement Process

Parameters	g2	G1	G2	G3
f (MHz)	501.76	501.13	501.006	501.13
R_S (M Ω)	6.38 (+13.3%)	6.43 (+14.26%)	6.39 (+13.34%)	5.63 (0)
P_m (W/cm ²)	7.97	8.91	7.497	3.16 (-39.20%)
Q	43686	42694	44357	49665
R/Q (Ω)	145.95	150.67	143.88	113.29
E_{max} (MV/m)	10.57	10.97	10.52	7.61

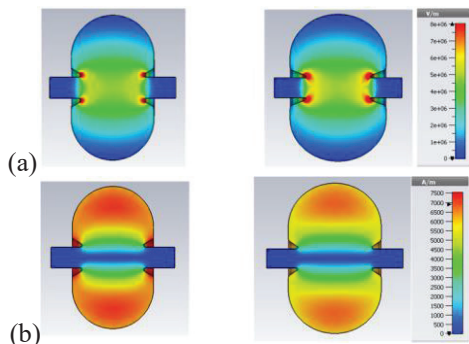


Figure 5: Comparison of field cloud plot. (a) E field of the original design and G2, (b) H field of the original design and G4.

The distribution of E fields are approximately the same while the exact values are different. Clear difference emerges between the H fields, which illustrate different modes exist in the cavities.

The shunt impedance is strongly dependent on the size of aperture, however, the beam pipe size cannot be changed randomly as it requires adaptability with the whole system. During further research, more focus will be laid on R/Q to improve the acceleration efficiency and controlling the peak field E_{max} below a certain threshold to avoid field breakdown for the main cavity.

DESIGN AND OPTIMIZATION OF THE HIGHER HARMONIC CAVITY

The original design of the HHC is carefully designed with the use of nose cones and the cavity shape maximizes the shunt impedance which result in a good improvement over pillbox or bell-shaped designs with the same bore. In correspondence with the physics requirement of ALS-U, the HHC would be more preferred if the previous R/Q of 80.4 Ω [8] reduce to around 30 Ω , thus a required-low and high Q elliptical shape cavity is designed and optimized in the preliminary stage. The parameterized sketch is shown in Fig. 6.

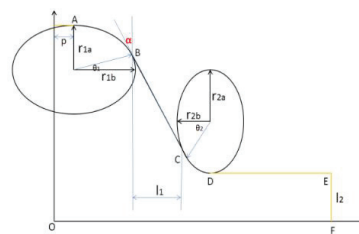


Figure 6: Geometry sketch of cavity shape for HHC.

Due to limitation of space and the consideration of transit time factor, the cavity length is added as a constraint with R/Q . The location of point D is considered as the right limit. Since the high Q nature of the super-conducting shape cavity, Q is not considered as an objective in this case. Though the algorithm, the Pareto front combined with Q is demonstrated in Fig. 7. Decreasing the cavity length leads to the sacrifice of a lower R/Q value. A trade-off is taken and the optimized results are chosen for further study. After evaluation a model is chosen as a base for further study shown in Fig. 8. Related study on beam dynamics requirements, higher order mode characterization and damping schemes are underway.

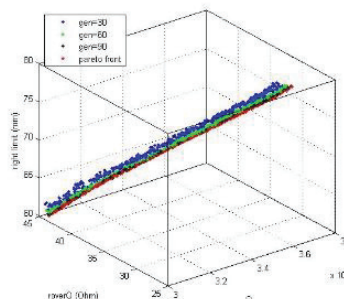


Figure 7: The converging process of R/Q , Q and the right limit with generations passing by.

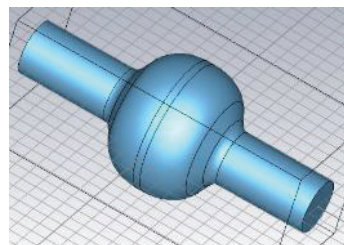


Figure 8: 3D model of one candidate geometry.

CONCLUSION

The design and optimization of a 500 MHz main cavity and a 1.5 GHz Higher harmonic cavity for ALS-U are presented in this paper. This RF cavity design method combines genetic algorithm, EM field solver and parallel computing, proving to be a very useful tool for the RF cavity design. The functional computational tool brings access to a wide range of study on optimization for complex systems and has great potential application to accelerator physics and engineering problems.

REFERENCES

- [1] C. Steier *et al.*, “Status of the Conceptual Design of ALS-U”, in *Proc. IPAC’18*, Vancouver, BC, Canada, Apr.-May 2018, pp. 4134-4137.
- [2] T. Luo *et al.*, “RF design of APEX2 two-cell continuous-wave normal conducting photo-electron gun cavity based on multi-objective genetic algorithm”, to be submitted.
- [3] T. Murata and H. Ishibuchi, “MOGA: multi-objective genetic algorithms”, *IEEE International Conference on Evolutionary Computation*, 1995.
- [4] K. Deb *et al.*, “A fast and elitist multiobjective genetic algorithm: NSGA-II”, *IEEE Transactions on Evolutionary Computation*, Volume: 6, Issue: 2, pp.182-197, 2002.
- [5] B. Taylor, K.Baptiste *et al.*, “The ALS storage ring RF system”, *Particle Accelerator Conference*, 1993.
- [6] Poisson/Superfish, Los Alamos Accelerator Code Group, <http://laacg.lanl.gov/>
- [7] CST, <https://www.cst.com>
- [8] R. A. Rimmer *et al.*, “The Third-Harmonic RF Cavity for the Advanced Light Source”, in *Proc. PAC’19*, New York, 1999, pp. 3131-3133.

Content from this work may be used under the terms of the CC BY 3.0 licence (© 2019). Any distribution of this work must maintain attribution to the author(s), title of the work, publisher, and DOI